Electronic Supplementary Information (ESI)

Electrolytic Synthesis of Porphyrinic Zr-Metal–Organic Frameworks with Selective Crystal Topologies

Keito Okada,[a] Yoko Tanaka,[a] Tomoko Inose,[b,c] Hiroshi Ujii,[b,d] Hirofumi Yoshikawa,[c] and Daisuke Tanaka*[a,f]

[a] *Department of Chemistry, School of Science and Technology, Kwansei Gakuin University, 2-1 Gakuen, Sanda, Hyogo 669-1337, Japan.*

[b] *Research Institute for Electronic Science (RIES), Hokkaido University, N20W10, Sapporo 001-0020, Japan*

[c] *Institute for Integrated Cell-Material Sciences (WPI-iCeMS), Kyoto University, Yoshida, Sakyo-ku, Kyoto 606-8501, Japan*

[d] *Department of Chemistry, KU Leuven, Celestijnenlaan 200F, Heverlee, 3001, Belgium*

[e] *Department of Nanotechnology for Sustainable Energy, School of Science and Technology, Kwansei Gakuin University, Sanda, Hyogo 669-1337, Japan*

[f] *JST PRESTO, 2-1 Gakuen, Sanda, Hyogo 669-1337, Japan*

**Corresponding Author. E-mail: dtanaka@kwansei.ac.jp.*

Table of Contents

S1. Materials and methods

Chemicals. Nitric acid (60%), acetic acid, *N,N*-dimethylformamide (DMF), ethanol (99.5%), and methanol were purchased from FUJIFILM Wako Pure Chemical Corporation. Distilled water was obtained from KISHIDA CHEMICAL Co., Ltd. Acetone was purchased from Kanto Chemical Co., Inc. All chemicals and solvents were of reagent grade and used without further purification. Zirconium plates (0.02×100×200 mm, 99.2%) were purchased from The Nilaco Corporation and cut into 10-mm squares. Pt/Ir wire (ratio 8:2, diameter 0.25 mm) was purchased from TANAKA Kikinzoku Kogyo K.K. and cut to an appropriate length. Tetrakis(4-carboxyphenyl)porphyrin (H_4TCPP) was purchased from Tokyo Chemical Industry Co., Ltd., and when required, it was also synthesized using a previously reported method.[1]

Methods. The zirconium plates and Pt/Ir wires were welded together using an ultra-small spot welding device (KTH-MWS, AS ONE Corporation). A stabilized DC power supply (AD-8723D, A&D Co., Ltd.) was used for the application of a constant current. Powder X-ray diffraction (PXRD) spectra were recorded on a Rigaku MiniFlex600 diffractometer at 40 kV and 15 mA using a Cu-target tube. The samples were examined without grinding, and the data were collected in the 2θ range of 2°–50° or 3°–50° using Cu–Kα radiation. Scanning electron microscopy (SEM) was performed on a JEOL JCM-6000 system. Nitrogen adsorption isotherms were obtained using a MicrotracBEL BELSORP-max volumetric gas adsorption measurement system. The samples were dried under reduced pressure at 150 °C for 12 h prior to use. Raman spectroscopy was conducted using a home-made, inverted optical microscope (Ti-U, Nikon) equipped with a piezoelectric stage (P517.3CL, PI), which was operated using an atomic force microscopy (AFM) controller (CombiScope TM 1000, Horiba). CW lasers of 532 nm were used as the excitation light. The laser light was focused on the sample by an objective (Plan Fluor 60x N.A. 0.85, Nikon) and scattered Raman emission was collected by the same objective. The Raman emissions were then guided to a spectrograph (iHR320, Horiba) equipped with a cooled-charge coupled device (CCD) (Newton 920P BRDD, Andor) after passing through a confocal pinhole (100 μm in diameter) and a long-path optical filter to remove excitation light (BLP01-532, SEMROCK, HQ655LP, CHROMA, or RET792LP, CHROMA, respectively). The obtained spectra were calibrated using toluene as the standard sample with a home-made MATLAB routine.

S2. Synthetic methods

Preparation of the anode. An anode was prepared by welding a Pt/Ir wire and a zirconium plate (10×10 mm^2) together using an ultra-small spot welding device. The anode was sonicated in acetone, distilled water, and then ethanol for 10 min each to remove any residue adhering to the substrate surface, such as organic matter. The washed anode was then dried by a nitrogen flow.

Electrolysis setup. The synthesis was performed under nitrogen using an electrolysis setup consisting of a two-necked eggplant-shaped flask containing the synthetic solution and two electrodes that were connected to a stabilized DC power supply with an output cable (Fig. S1). The two electrodes were immersed in the synthetic solution and fixed at a distance of approximately 15 mm using a septum. The set-up was heated in an oil bath.

Synthesis procedure under condition A. H_4TCPP (199 mg) was dissolved in 25 mL of DMF, followed by the addition of nitric acid (300 µL), water (90 µL), and acetic acid (715 µL). The electrodes were immersed in the resulting solution and heated to 110 °C under a nitrogen atmosphere. Purple crystals were deposited onto the anode and precipitated in solution after applying a constant current of 30 mA for a certain time period (3 min, 1 h, 2 h, or 3 h). The synthetic solution was cooled, and the synthesized anode substrate was removed from the reaction vessel and immersed in DMF to remove any residual H_4TCPP. The anode substrate was then washed with methanol. The crystals that precipitated in the solution were filtered and washed with DMF and methanol. The anode substrate and the crystals were then air-dried at room temperature.

Synthesis procedure under condition B. H_4TCPP (425 mg) was dissolved in 25 mL of DMF, followed by the addition of nitric acid (300 µL), water (90 µL), and acetic acid (13.3 mL). After that, synthesis was performed following the procedure used under condition A.

Synthesis procedure under condition C. H_4TCPP (425 mg) was dissolved in 25 mL of DMF, followed by the addition of nitric acid (300 µL), water (90 µL), and acetic acid (715 µL). After that, synthesis was performed following the procedure used under condition A.

Synthesis procedure under condition D. H_4TCPP (199 mg) was dissolved in 25 mL of DMF, followed by the addition of nitric acid (300 µL), water (90 µL), and acetic acid (13.3 mL). After that, synthesis was performed following the procedure used under condition A.

Calculation of yields. Yields were calculated using methods similar to those previously reported.[2] While calculating the yields, it was assumed that the Zr-metal substrate was converted to Zr(IV) ions during electrolysis with 100% Faraday efficiency. In addition, it was assumed that all crystals obtained under conditions A and B were PCN-222 and PCN-224, respectively. The compositions of PCN-222 and PCN-224 are summarized in Table S1. The amounts and yields of the compounds formed on the anode and in the solution after electrolysis under each condition for 2 h are summarized in Table S2. The yields of PCN-222 and PCN-224 obtained by electrolytic synthesis were lower than the reported values of PCN-222 and PCN-224 synthesized by the solvothermal method (Table S3).[3,4]

Table S1. Compositions of PCN-222 (no metal) and PCN-224 (no metal).

Compound	Composition
PCN-222 (no metal)	$(C_{48}H_{34}N_4O_{16}Zr_3)_n$
PCN-224 (no metal)	$(C_{144}H_{122}N_{12}O_{64}Zr_{12})_n$

Table S2. Actual amounts and yields of the products obtained after electrolysis under conditions A and B for 2 h.

	Cond. A_2 h	Cond. B_2 h
Actual amount of crystals on the anode	19.6 mg	12.5 mg
Actual amount of crystals in the solutions	20.7 mg	14.1 mg
Total actual amount	40.3 mg	26.6 mg
Yield of the crystals on the anode	8.7%	6.5%
Yield of the crystals in the solutions	9.3%	7.3%
Total yield	18.1%	13.8%

Table S3. Yields of PCN-222 and PCN-224 synthesized by electrolytic synthesis and previously conducted solvothermal syntheses.[3,4]

	Yield / %
Reported yield of PCN-222 by solvothermal method	46
Reported yield of PCN-224 by solvothermal method	71
Yield of PCN-222 by electrolysis method	18.1
Yield of PCN-224 by electrolysis method	13.8

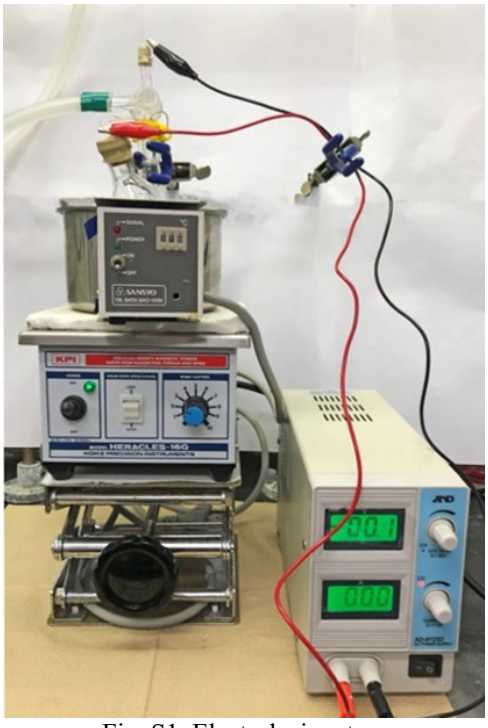

Fig. S1. Electrolysis setup.

S3. Electrolytic synthesis of porphyrinic Zr-MOFs at low temperature

The electrolytic synthesis experiments were conducted at a low temperature of 60 °C under conditions A and B to investigate the influence of temperature on the formation process of PCN-222 and PCN-224. Since the anodes obtained under both conditions had only small deposits, the anodes were analyzed by PXRD as substrates without further processing (Fig. S2). From the PXRD pattern, no MOF-derived peaks were observed under the low-temperature conditions, indicating that high temperature is important for the successful crystallization of porphyrinic Zr-MOFs. The synthetic temperature in this experiment (110 °C) is a high-temperature condition that is already above the boiling points of water (100 °C) and nitric acid (83 °C) under ambient pressure. Hence, temperatures higher than 110 °C could not be examined in this experiment because they would exceed the boiling point of acetic acid (118 °C).

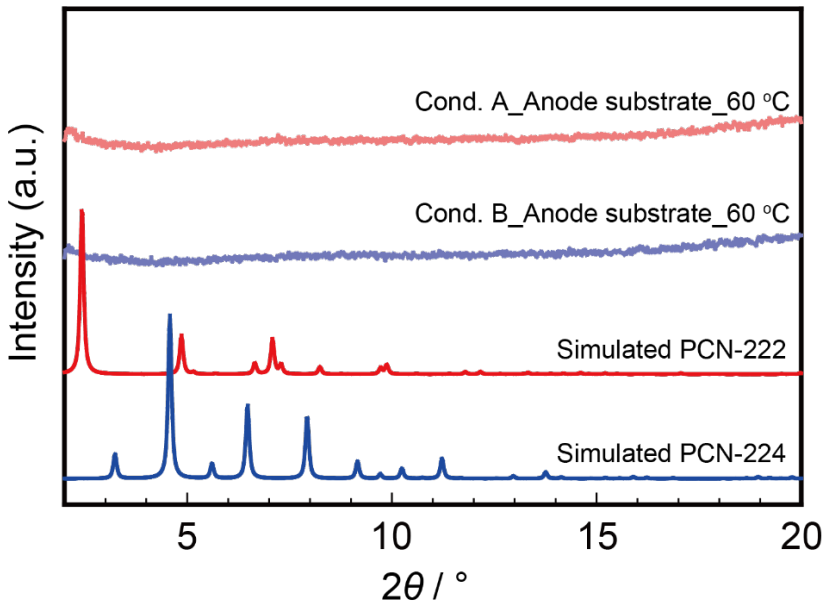

Fig. S2. The powder X-ray diffraction (PXRD) patterns of anodes obtained after electrolytic synthesis at low temperature under conditions A and B.[3,4]

S4. Synthesis experiments without applied current

Zr metal is likely to react with acids and linkers without applied current. Therefore, experiments without applied current under conditions A and B were carried out, and PXRD measurements of the obtained anodes were performed (Fig. S3). The PXRD patterns revealed that no crystalline material had formed without applied current.

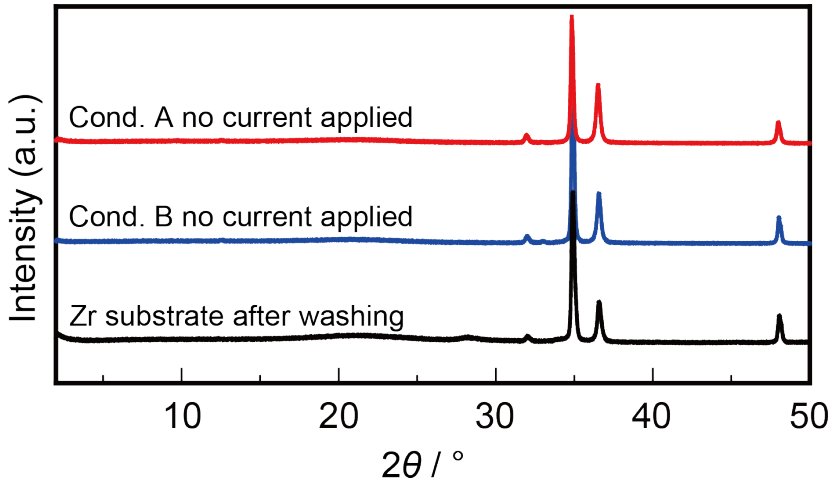

Fig. S3. The PXRD patterns of the anodes after experiments were performed under conditions A and B without applied current.

S5. PXRD patterns of the crystals on the anode and in the solution

The crystals deposited on the anode after electrolysis for 2h under conditions A through D were peeled off of the anode substrate and analyzed by PXRD. The crystals that formed in solution under conditions A and B were also analyzed. The PXRD patterns of the crystals deposited on the anode and precipitated in the solution are shown in Figs. S4 and S5, respectively.

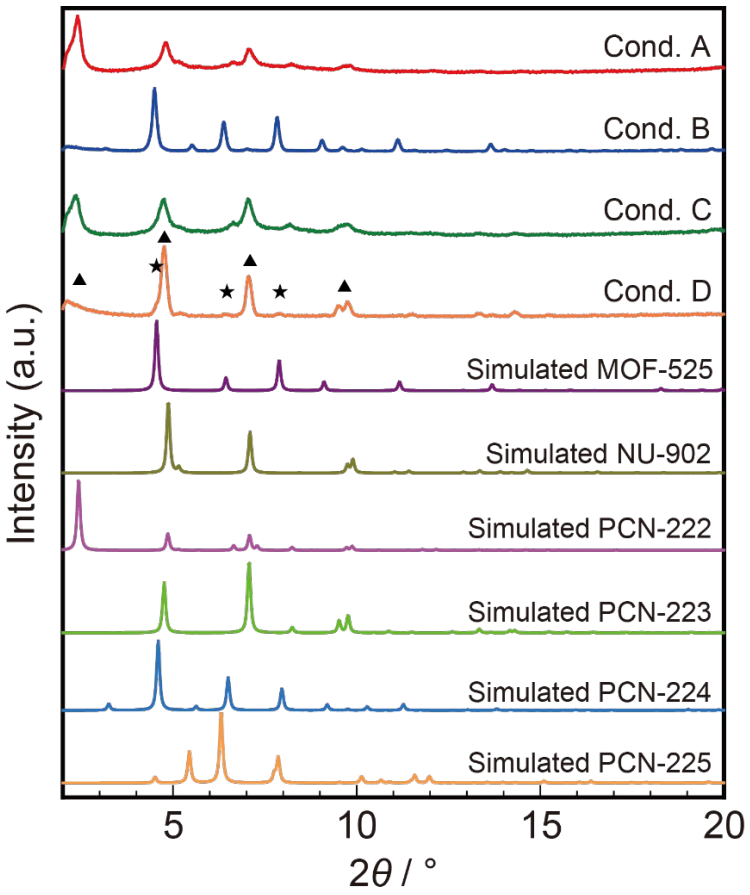

Fig. S4. PXRD patterns of the crystals deposited on the anode under conditions A through D, along with the simulated XRD patterns of the six crystal topologies of porphyrinic Zr-MOFs.[3–8] The black triangles on the PXRD pattern of condition D indicate peaks derived from PCN-222, PCN-223 or NU-902, and the black stars indicate peaks derived from PCN-224 or MOF-525.

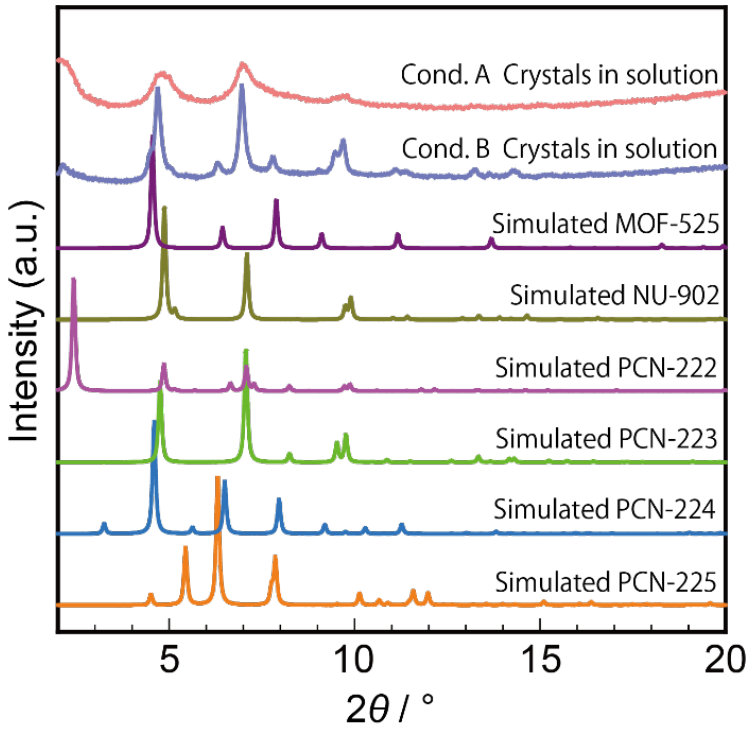

Fig. S5. PXRD patterns of the crystals formed in solution under conditions A and B, and the simulated XRD patterns of the six crystal topologies of porphyrinic Zr-MOFs.[3–8]

S6. Nitrogen gas adsorption measurements

The pores of the crystals obtained after 2 h of electrolysis under conditions A and B were analyzed by nitrogen gas adsorption measurements at 77 K. The results of the nitrogen adsorption measurements and the Brunauer–Emmett–Teller (BET) surface areas determined from the isotherms are shown in Fig. S6 and Table S4, respectively. The samples were peeled off of the anode prior to analysis. The onset pressure and step position of the isotherms are the same as those previously reported for the known compounds, suggesting that PCN-222 and 224 were in fact obtained.

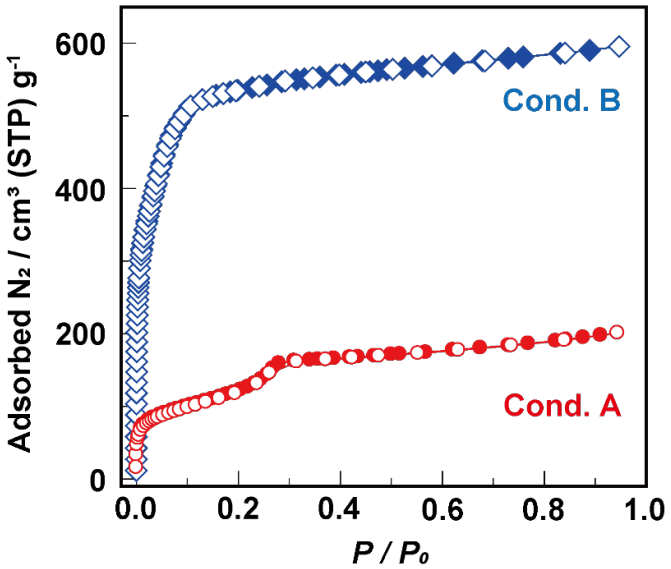

Fig. S6. Nitrogen gas adsorption isotherms of the crystals deposited on the anode under conditions A and B after electrolysis was conducted for 2 h.

Table S4. Isotherm types and BET surface areas of samples obtained under conditions A and B and those previously reported for PCN-222 and PCN-224.[3,4]

	Isotherms type	BET surface area / m^2 g^{-1}
Cond. A	Type IV	419
PCN-222 (reported)	Type IV	2200
Cond. B	Type I	2093
PCN-224 (reported)	Type I	2600

S7. Improvement in the crystallinity of PCN-222 by extending the heating time

As shown in the schemes of Figs. 4a and b, PCN-222 is thought to be formed by a gradual phase change via an amorphous phase during the electrolytic synthesis. However, since long-term electrolysis causes the anode substrate to deteriorate, improvements in crystallinity were not expected to be accomplished by long-term electrolytic synthesis. On the other hand, a previous paper on the synthesis of porphyrin Zr-MOFs by a solution stirring method reported that PCN-222 was obtained as the main product via a synthesis employing a high temperature and long reaction time.[9] It is also expected that the crystallinity of the deposits on the substrate will be improved by stopping the voltage application after electrolysis and extending only the heating time. Therefore, under the conditions that provided PCN-222 (condition A), an experiment was conducted where only the heating time was extended after the electrolytic reaction was completed. Specifically, after 2 h of electrolysis the heating of the reaction solution at 110 °C continued for 1 or 7 days. Subsequently, the obtained crystals were peeled off of the anode substrate and analyzed by PXRD and nitrogen adsorption measurements. The PXRD patterns and nitrogen adsorption isotherms of the crystals obtained under extended heating times are shown in Figs. S7a and b, respectively. The PXRD patterns of the crystals that had been obtained after additional heating (1 day or 7 days) after electrolysis exhibited slightly sharper peaks than those of the crystals obtained directly after electrolysis without additional heating. These sharper peaks suggested that the crystallinity was improved by the extended heating conditions. The nitrogen adsorption isotherms revealed that the amount of nitrogen adsorbed by the crystals heated for 7 days was significantly higher than that by the crystals without additional heating. Furthermore, the BET surface areas of the crystals heated for 7 days after electrolysis were about 2.5 times greater than those of the crystals without additional heating (Table S5). Although the crystallinity of PCN-222 obtained by electrolysis was lower than that of PCN-222 obtained by solvothermal synthesis, it was suggested that the crystallinity could be improved by post-electrolysis treatments, such as extended heating.

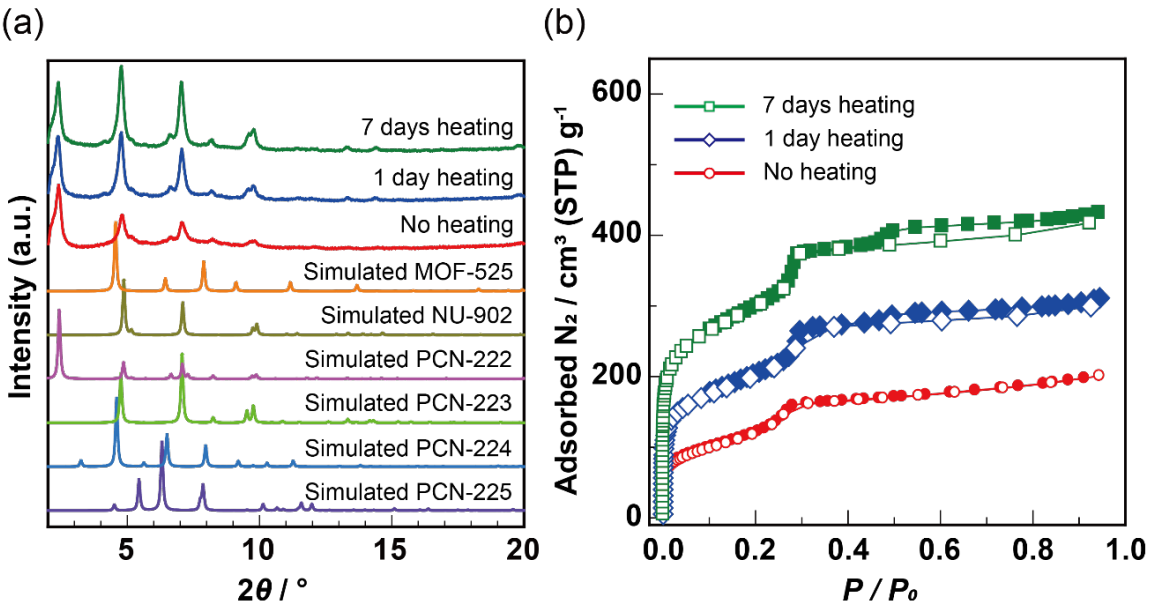

Fig. S7. (a) PXRD patterns and (b) nitrogen adsorption isotherms of crystals obtained on the anode upon extended heating after electrolysis.[3–8]

Table S5. BET surface areas of PCN-222 obtained before and after extended heating times and that previously reported for PCN-222 obtained via solvothermal synthesis.[4]

	BET surface area / m^2 g^{-1}
PCN-222 by reported solvothermal synthesis	2200
PCN-222 by electrolysis (no heating)	419
PCN-222 by electrolysis (1 day heating)	713
PCN-222 by electrolysis (7 days heating)	1047

S8. PXRD patterns of the samples obtained during time modulation experiments

The time modulation experiments were performed under conditions A and B and the resultant crystals obtained on the anodes were analyzed by PXRD (Figs. S8 and S9, respectively). The samples obtained after conducting electrolysis for 3 min were examined without further processing; however, those obtained after 1 h were peeled off of the anode prior to analysis.

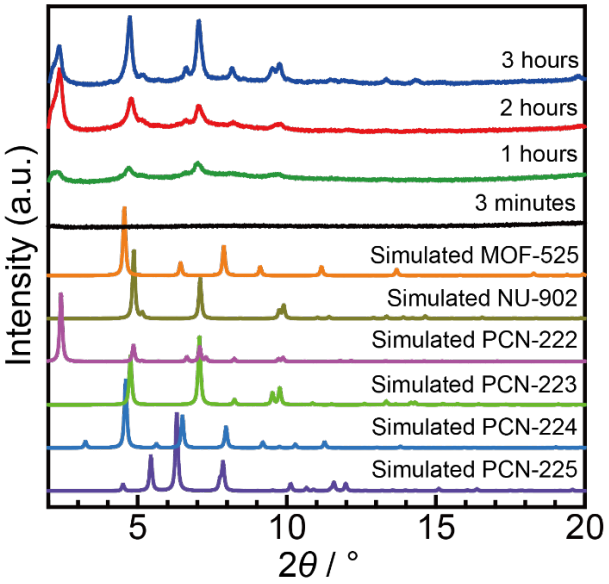

Fig. S8. PXRD patterns of the crystals deposited on the anode under condition A after various reaction times, and the simulated XRD patterns of the six crystal topologies reported for porphyrinic Zr-MOFs.[3–8]

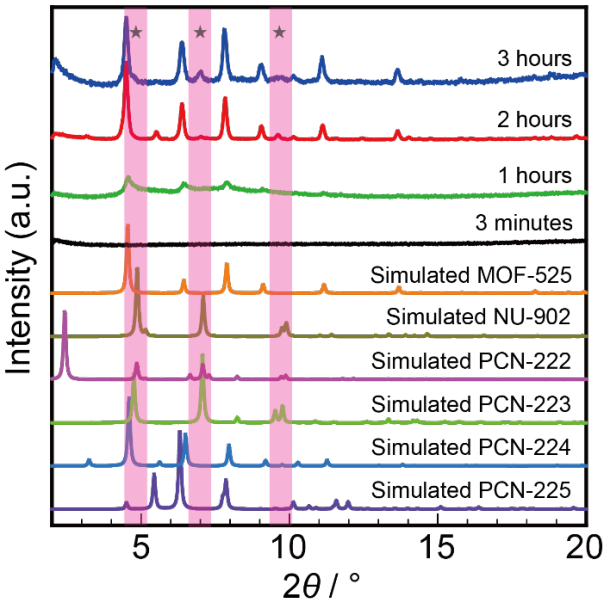

Fig. S9. PXRD patterns of the crystals deposited on the anode under condition B after various reaction times, and the simulated XRD patterns of the six crystal topologies reported for porphyrinic Zr-MOFs.[3–8]

S9. Raman spectroscopic data

The surface states of the substrates were analyzed by Raman spectroscopy. The Raman spectra of the samples obtained after 3 min and 2 h under each condition, along with that of H_4TCPP (ligand), are shown in Fig. S10. Table S6 shows the functional groups and vibrational modes of the main peaks assigned from the obtained Raman spectra.[10–12] The samples obtained after 3 min were examined without further processing, while those obtained after 2 h were peeled off of the substrate prior to analysis.

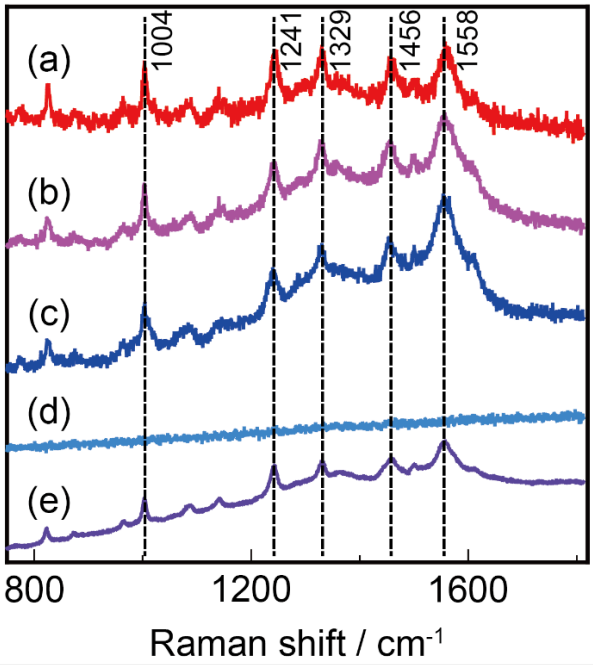

Fig. S10. Raman spectra of (a) PCN-222 crystals formed under condition A after 2 h, (b) the anode substrate obtained under condition A after 3 min (amorphous), (c) PCN-224 crystals formed under condition B after 2 h, (d) the anode substrate obtained under condition B after 3 min (no deposition), and (e) H_4TCPP.

Table. S6. The functional groups and vibrational modes of the main peaks assigned from the obtained Raman spectra.[10–12]

Raman shift	Functional group / Vibration mode
1004 cm^{-1}	In-plane bending deformation of phenyl ring
1241 cm^{-1}	Stretching mode between the *meso*-C and phenyl groups
1329 cm^{-1}	Symmetric ring mode of the porphyrin
1456 cm^{-1}	Symmetric ring mode of the porphyrin
1558 cm^{-1}	Symmetric ring mode of the porphyrin

References

1. S. Yuan, J. S. Qin, L. F. Zou, Y. P. Chen, X. Wang, Q. Zhang and H. C. Zhou, *J. Am. Chem. Soc.*, 2016, **138**, 6636-6642.
2. A. Martinez Joaristi, J. Juan-Alcañiz, P. Serra-Crespo, F. Kapteijn and J. Gascon, *Cryst. Growth Des.*, 2012, **12**, 3489-3498.
3. D. Feng, W. C. Chung, Z. Wei, Z. Y. Gu, H. L. Jiang, Y. P. Chen, D. J. Darensbourg and H. C. Zhou, *J. Am. Chem. Soc.*, 2013, **135**, 17105-17110.
4. D. Feng, Z. Y. Gu, J. R. Li, H. L. Jiang, Z. Wei and H. C. Zhou, *Angew. Chem., Int. Ed. Engl.*, 2012, **51**, 10307-10310.
5. P. Deria, D. A. Gomez-Gualdron, I. Hod, R. Q. Snurr, J. T. Hupp and O. K. Farha, *J. Am. Chem. Soc.*, 2016, **138**, 14449-14457.
6. D. Feng, Z. Y. Gu, Y. P. Chen, J. Park, Z. Wei, Y. Sun, M. Bosch, S. Yuan and H. C. Zhou, *J. Am. Chem. Soc.*, 2014, **136**, 17714-17717.
7. H. L. Jiang, D. Feng, K. Wang, Z. Y. Gu, Z. Wei, Y. P. Chen and H. C. Zhou, *J. Am. Chem. Soc.*, 2013, **135**, 13934-13938.
8. W. Morris, B. Volosskiy, S. Demir, F. Gandara, P. L. McGrier, H. Furukawa, D. Cascio, J. F. Stoddart and O. M. Yaghi, *Inorg. Chem.*, 2012, **51**, 6443-6445.
9. X. Gong, H. Noh, N. C. Gianneschi and O. K. Farha, *J. Am. Chem. Soc.*, 2019, **141**, 6146-6151.
10. M. Aydin, *Vib. Spectrosc.*, 2013, **68**, 141-152.
11. G. S. Saini, *Spectrochim. Acta, Part A*, 2006, **64**, 981-986.
12. P. Zardi, E. Gallo, G. A. Solan and A. J. Hudson, *Analyst*, 2016, **141**, 3050-3058.